Thermochimica Acta 474 (2008) 52–56

Contents lists available at ScienceDirect

Thermochimica Acta

journal homepage: www.elsevier.com/locate/tca

Density and phase diagram of the magnesium–lead system in the region of Mg_2Pb intermetallic compound

Sergei V. Stankus*, Rashid A. Khairulin

Institute of Thermophysics, Siberian Brunch of the Russian Academy of Sciences, Lavrentyev Avenue, 1, 630090 Novosibirsk, Russian Federation

ARTICLE INFO

Article history:
Received 1 April 2008
Received in revised form 16 May 2008
Accepted 20 May 2008
Available online 7 June 2008

Keywords:
Magnesium–lead system
Phase diagram
Density
Thermal analysis

ABSTRACT

The phase diagram of magnesium–lead system has been investigated by a new method for phase analysis on the basis of a strong penetrating radiation. The measurements have shown that the standard phase diagram of this system contains inaccuracy in the region of the Mg_2Pb intermetallic compound. New data on the temperature dependences of the solid and the melt densities have been obtained. The density change during the phase transitions has been directly measured.

1. Introduction

The equilibrium phase diagram of the magnesium–lead system has been studied extensively, and the data of most investigations are in good agreement. From the analysis of these investigations Nayeb-Hashemi and Clark [1] recommended the phase diagram (Fig. 1) that was used in reference books, including the one published recently [2]. However, the results of studies [3,4] are in contradiction with the recommendations of the analysis [1]. Eldridge et al. [3] have found that the Mg_2Pb intermetallic phase melts incongruently. Congruent melting is observed for a previously unknown β′-phase, at a composition which slightly differs from Mg_2Pb (Fig. 2). The authors of the survey [1] have reasoned that this result is in error and have given a detailed argumentation of this conclusion. The aim of the present work is a refinement of the phase diagram of the magnesium–lead system, and the application of a new method for phase analysis on the basis of a strong penetrating radiation.

2. Experimental details

The gamma method has been long used for the investigation of substances and materials density in both the solid and liquid states [5–8]. It is based on measuring the attenuation of a narrow beam of gamma quanta passing through a sample:

$$J(T) = J_0(T)\ \exp[-\mu\rho(T)l(T)], \tag{1}$$

where ρ is the density, T is the temperature, J and J_0 are the intensities of the radiation after passage through the experimental apparatus with and without the sample, respectively, l is the attenuation length, and μ is the mass attenuation coefficient of the investigated substance, which depends only on its chemical composition. From Eq. (1), it is evident that any change in the state of a substance, which is accompanied by a variation of its density, causes a change in the measured intensity (Fig. 3). The sensitivity of the gamma method of phase analysis is restricted by the random character of radioactive decay from the source. The process of radioactive decay obeys Poisson's distribution. The dispersion of the measured value of intensity σ^2 may be written as [9]:

$$\sigma^2 = J\tau, \tag{2}$$

where τ is the time of gamma quanta counting. Assuming that the root-mean-square deviation σ is the limit accuracy of the intensity measurement, the expression for the least density change that can be resolved by the gamma method is easy to obtain from Eqs. (1) and (2):

$$\frac{\Delta\rho}{\rho} = \frac{1}{\mu\rho l}\frac{1}{\sqrt{J\tau}} \tag{3}$$

* Corresponding author. Tel.: +7 383 3360706; fax: +7 383 3308480.
E-mail address: stankus@itp.nsc.ru (S.V. Stankus).

0040-6031/$ – see front matter © 2008 Elsevier B.V. All rights reserved.
doi:10.1016/j.tca.2008.05.011

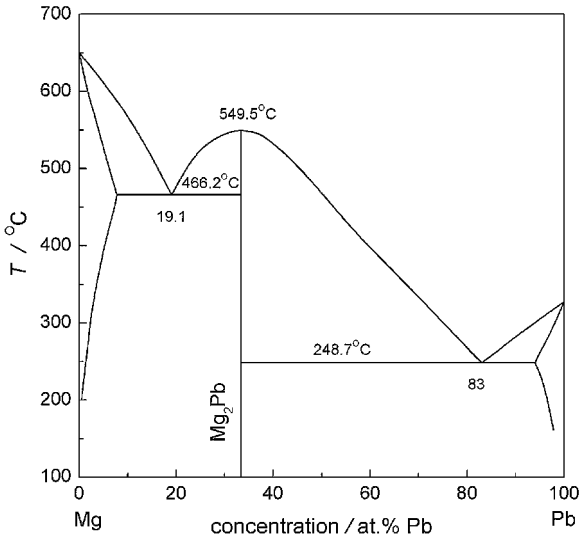

Fig. 1. The standard phase diagram of the magnesium–lead system.

The analysis of Eq. (3) shows that the highest sensitivity is achieved at $\mu\rho l = 2$. In this case, the Eq. (3) can be transformed to

$$\frac{\Delta\rho}{\rho} = 1.36\frac{1}{\sqrt{J_0\tau}} \tag{4}$$

For our installation, $J_0 \sim 50{,}000\ s^{-1}$, $\tau = 100$ s ($\Delta\rho\backslash\rho$) = 0.06%.

It should be pointed out that the gamma method does not require heating or cooling of a sample with terminal velocity, and thus it can be used for the investigation of an isothermal process in contrast to most other methods of thermal analysis. In addition, an analysis of the gamma experiments allows the obtaining of information about the density and thermal expansion coefficient (CTE) of a substance both in the solid ρ_c and liquid ρ_m states, and also to obtain information about density changes on phase transitions. This allows a judgment of the structure of the melts and solids, which is especially important for metastable phases that exist within a narrow temperature range. According to [6]:

$$\rho_m(T) = \frac{\ln[J_0(T)/J(T)]}{\mu l_{20}[1+\bar{\alpha}(T)(T-20)]} \tag{5}$$

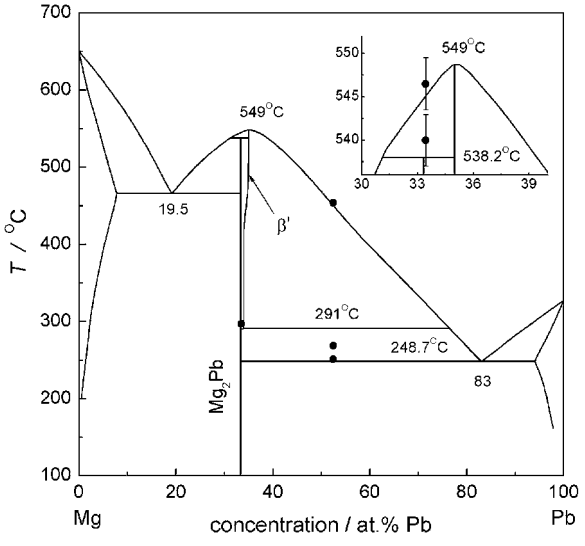

Fig. 2. The alternative phase diagram of the magnesium–lead system [3]. Points are the results of this research.

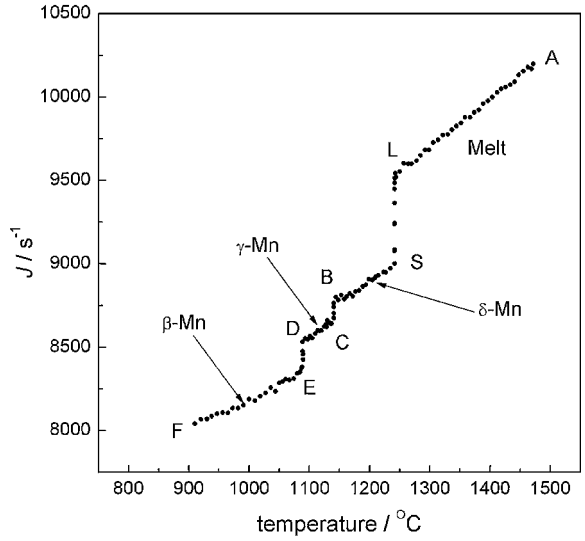

Fig. 3. Temperature dependence of the radiation intensity (gammagram) after passage through the sample of manganese on cooling from 1475 °C. AL is the liquid state, LS is the crystallization, SB is the δ-phase, CD is the γ-phase, and EF is the β-phase.

$$\rho_c(T) = \rho_r(T_r)\left\{\frac{\ln[J_0(T)/J(T)]}{\ln[J_0(T_r)/J(T_r)]}\right\}^{3/2} \tag{6}$$

$$\delta\rho_{LS} = \frac{\rho_c(T_S)-\rho_m(T_L)}{\rho_c(T_S)} = 1 - \frac{\ln[J_0(T_L)/J(T_L)]}{\ln[J_0(T_S)/J(T_S)]} \tag{7}$$

$$\delta\rho_{trs} = \frac{\rho_c(T_{trs}^-)-\rho_c(T_{trs}^+)}{\rho_c(T_{trs}^-)} = 1 - \left\{\frac{\ln[J_0(T_{trs}^+)/J(T_{trs}^+)]}{\ln[J_0(T_{trs}^-)/J(T_{trs}^-)]}\right\}^{3/2} \tag{8}$$

Here, T is temperature in °C; l_{20} is the attenuation length at 20 °C; $\bar{\alpha}(T)$ is the mean linear coefficient of thermal expansion of the cell material; ρ_r is the density at T_r temperature; $\delta\rho_{LS}$ and $\delta\rho_{trs}$ are the relative density changes on melting and solid phase transition, respectively; the subscripts L and S are used to denote the values relating to the liquidus and solidus, respectively; T_{trs} is the temperature of the solid phase transition; and the superscripts (−) and (+) are used to denote the values relating to the low-temperature and high-temperature solid phases, respectively. The Eqs. (6) and (8) are valid for isotropic materials. The $J_0(T)$ dependence is determined in the calibration experiment. The reference density, ρ_r, can be measured by an independent method, or it is calculated using Eq. (5). The mass attenuation coefficient of multicomponent systems can be found from the formula:

$$\mu = \sum \mu_i c_i, \tag{9}$$

where μ_i and c_i are the mass attenuation coefficients and the mass concentrations of the elements in the alloy, respectively.

The measurements have been carried out with a γ-densitometer P-3 of the Thermophysics Institute of the Siberian Branch of the Russian Academy of Sciences. A basic scheme of the experimental set-up is shown in Fig. 4. An isotope of caesium 137 with an activity of about 50 GBq was used as the source for gamma quanta. The high-temperature electric furnace consists of water-cooled base (q) electric inlets (u), cap (g) with a flange (h) for connection of the vacuum and gas lines, a support with thermostating block (l), heaters (m, t) and the heat shield systems (j, n, s). The block is made as a thick-walled copper sleeve (96 mm in diameter and 110 mm in height) with a cover (k). A crucible with the substance under investigation (d) is placed into a hole of 56-mm diameter and 110-mm depth. The block is set upon the stainless steel support with an 150 W additional heater (t). The main heater (m) with 0.05 Ω resis-

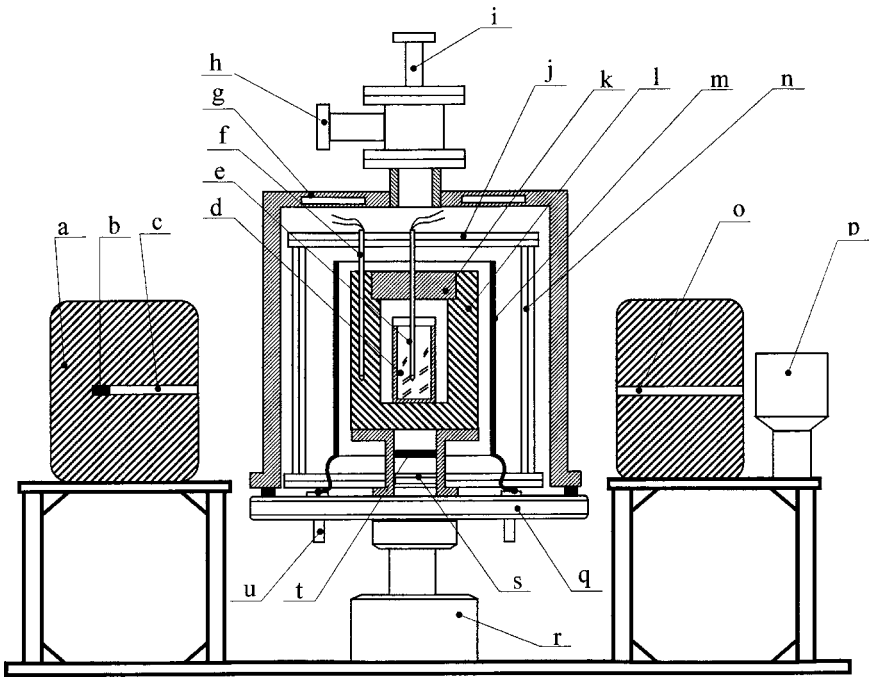

Fig. 4. The basic scheme of the gamma densitometer P-3. *The letters in the scheme represent the following in corresponding order:* (a) block of biological protection; (b) gamma ray source (^{137}Cs); (c and o) collimators; (d) crucible with the investigated substance; (e) main thermocouple; (f) one of the control thermocouples; (g) water-cooled cap; (h) flange for connection of the vacuum and gas lines; (i) mechanical mixer; (j, n, and s) systems of heat shields; (k) cover of the block; (l) thermostating block; (m) basic heater; (p) scintillation counter; (q) water-cooled basin; (r) lifting gear; (t) additional heater; and (u) electric inlets.

tance is made from stainless steel. The operating temperature range is 20–850 °C, and the power consumption does not exceed 3 kW. The measurements can be carried out in vacuum up to 10 mPa or in an argon atmosphere at pressures up to 0.3 MPa. The control system enables the change in temperature at a rate from 0.2 to 5 °C/min, and also holds a constant temperature with an error of no more than 0.1 °C. In the last case, the temperature difference on the interior surface of the block does not exceed 0.5 °C. The temperature is measured by a K-type thermocouple (e), which is placed directly into the sample in the protective sleeve. In addition, four thermocouples (f) measure the temperatures of the copper block and support. They are used for adjustment, recording the thermogram, and checking the temperature gradient.

The analysis of the available data has shown that the reliability of the results from investigating the properties and phase diagrams of binary and multicomponent systems depends significantly on the sample states [8]. So, considerable errors in determination of the temperatures of phase equilibrium can be observed in the presence of a concentration gradient in the sample. The diameter of the radiation beam (4 mm) is much less than the typical height of a sample (30–60 mm). Therefore, it is possible to check the homogeneity of the samples in both the solid and liquid states by measuring the intensity J as a function of the distance from the crucible bottom (h). Towards this purpose, the installation was equipped with a mechanical mixer (i) for stirring the melt and a lifting gear for the vertical movement of the furnace (r) with respect to the gamma quanta beam.

The computer-based system of data collection and processing records the intensity J and the emf of two thermocouples every 10 s. It enables the recording of the gammagram (temperature dependence of the intensity), the thermogram (time dependence of the sample temperature), and the analogue of the DTA thermogram (the temperature dependence of the temperature difference between the sample and copper block), simultaneously.

Cylindrical tantalum crucibles of 26–30-mm diameter and 60-mm height, with a cover and a thin-walled protective sleeve for the thermocouple, were used. The temperature was measured by the chromel–alumel thermocouples, which were checked against the melting points of pure tin and antimony. The deviations of the measured melting temperatures from the reference data did not exceed 1 °C. Before the experiments, the furnace of the gamma densitometer was evacuated and filled with pure argon (99.992 vol.%) up to 0.1 MPa. Measurements were mainly conducted at a heating/cooling rate of 1–5 °C/min. The density of the samples at room temperature was determined by the Archimedean method with an error of no more than 0.05%. The mass attenuation coefficients of magnesium (0.00764 m^2/kg) and lead (0.01090 m^2/kg) were measured directly in the installation. According to our estimate, the density measurement error did not exceed 0.20–0.25% at the maximum temperature of the experiments.

The samples were synthesized directly in the experiments by melting magnesium and lead weights in the required ratio. Thereafter, the melt was stirred thoroughly with a mechanical mixer. The purity of the components was 99.95% (Mg, Solikamskii Magnesium Factory) and 99.99% (Pb, Yuzhpolimetall). The homogeneity of the liquid alloys was controlled by measuring the radiation intensity at different distances between the beam axis and crucible bottom. The measurements were carried out only on cooling of the samples. Alloys with lead content of 33.45 and 52.46 at.% were studied. The concentration error did not exceed 0.06–0.08%.

3. Results and discussion

A gammagram and a DTA thermogram of the sample with 33.45 at.% Pb content obtained on cooling at a rate of 3 °C/min are shown in Figs. 5 and 6. As illustrated in Fig. 5, there are two peaks of exothermic reactions in the temperature range of 475–600 °C, which begin at:

$$T_L = 546.5 \pm 3\,^{\circ}C \quad \text{and} \quad T_B = 540 \pm 3\,^{\circ}C \tag{10}$$

At the same temperatures on the gammagram, there is an abrupt intensity decrease (increase of the density), followed by an increase.

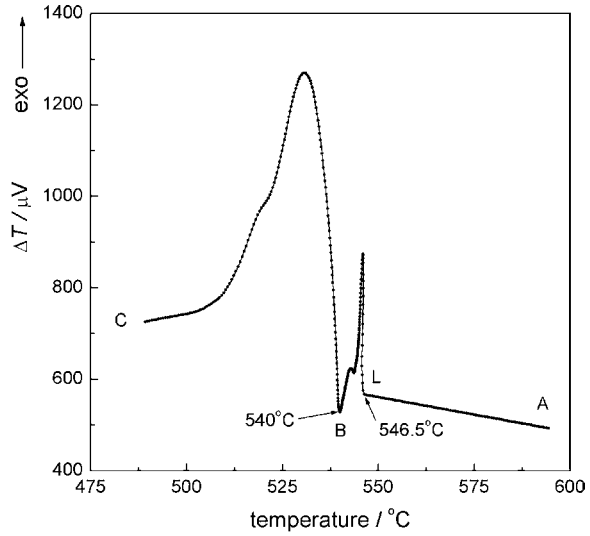

Fig. 5. DTA thermogram obtained on the cooling of the sample with 33.45 at.% Pb content. ΔT is the temperature difference between the sample and block.

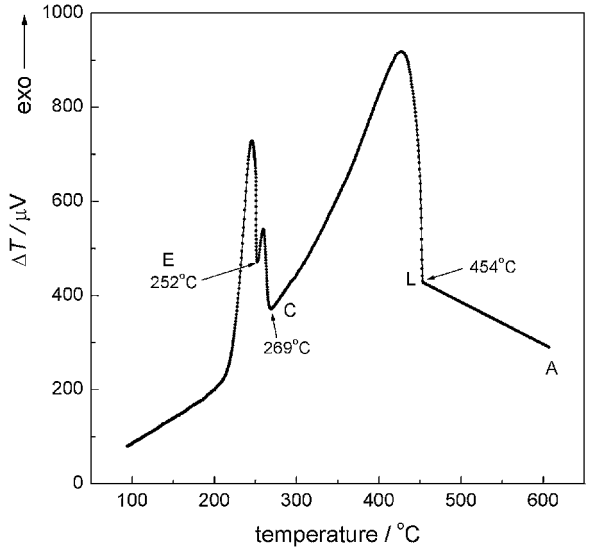

Fig. 7. DTA thermogram obtained on the cooling of the sample with 52.46 at.% Pb content. ΔT is the temperature difference between the sample and block.

In addition, a density decrease of 1.5% for the sample is observed at:

$$T_C = 297 \pm 3\,^{\circ}C \quad (11)$$

It is impossible to explain such phase changes of the sample using the standard phase diagram shown in Fig. 1. However, they correspond to the alternative phase diagram (Fig. 2). According to the latter, a crystallization of β′-phase takes place on LB. Our measurements show that the β′-phase is essentially more dense than the melt.

A peritectic reaction:

$$\text{melt} + \beta' \rightarrow Mg_2Pb + \beta' \quad (12)$$

begins at T_B with the Mg_2Pb phase having a smaller density than β′. The latter phase exists in a restricted temperature range, and it decomposes into Mg_2Pb and a little amount of the melt at T_C. The composition of the liquid phase is close to the composition of the low-temperature eutectic. The investigation of a sample containing 52.46 at.% Pb (Figs. 7 and 8) confirms the correctness of the alternative phase diagram of the magnesium–lead system. The melt crystallization (Fig. 8) begins at:

$$T_L = 454 \pm 3\,^{\circ}C \quad (13)$$

Then the sample state changes according to the reaction:

$$\text{melt} + \beta' \rightarrow \text{melt} + Mg_2Pb \quad (12)$$

at

$$T_C = 269 \pm 3\,^{\circ}C \quad (15)$$

Residues of the liquid phase crystallize into the low-temperature eutectic with an increase in density at:

$$T_E = 251 \pm 3\,^{\circ}C. \quad (16)$$

The temperatures of the phase changes according to Eqs. (10), (11), (13), and (16) agree with previous data [3,4] within the estimated error (Fig. 2). The temperature obtained from Eq. (15) is a little

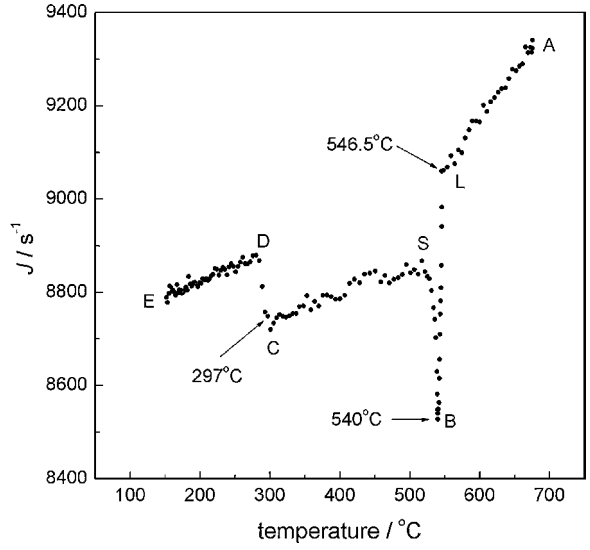

Fig. 6. Gammagram obtained on the cooling of the sample with 33.45 at.% Pb content.

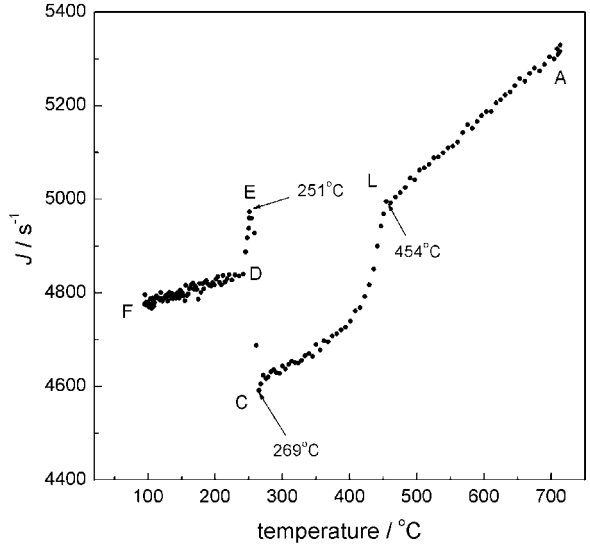

Fig. 8. Gammagram obtained on the cooling of the sample with 52.46 at.% Pb content.

lower than that from Eq. (11). This is probably due to kinetic reasons, namely difficult nucleation of the Mg_2Pb phase. A wide scatter of this temperature was also observed in [3]. Moreover, it was observed in [10] that the initial stage of the low-temperature eutectic crystallization also occurred in the β′-phase [10]. Notice that in all the cases, the data of the gamma analysis differ from those of the thermal analysis by no more than 1°.

The results obtained allow the calculation of the density of all phases and the volume changes on transitions between them using the Eqs. (5)–(8). The density of the homogeneous liquid alloy at T_L was accepted as the reference density, which was calculated from Eq. (5). The data processing for the existence interval of the Mg_2Pb phase (ED in Fig. 6) has given the equation:

$$\rho_{Mg_2Pb}(T) = 5389 - 0.31081\,(T - 20\,^{\circ}\mathrm{C})\ \text{in}\ \mathrm{kg/m^3} \quad (17)$$

The confidence bounds (95%) of the density random error are equal to ±0.10%. The total errors essentially exceed this value because a concentration gradient (0.12 %/mm) is observed in the sample, and completeness of the β' → Mg_2Pb transition (CD in Fig. 6) has not been controlled. Nevertheless, the experimental density of the Mg_2Pb phase at room temperature differs from the average X-ray density [11,12] by less than 0.02%. The extrapolation of Eq. (17) to the liquidus temperature gives a value that agrees with the melt density (ρ_L = 5256 kg/m^3 [13]) within the estimated error. It implies that the melting of the Mg_2Pb phase is accompanied by an insignificant volume change.

The temperature dependence of density over the interval CS in Fig. 6 is described by the equation:

$$\rho_{CS}(T) = 5384.6 - 0.26816\,(T - 297\ ^{\circ}\mathrm{C})\ \text{in}\ \mathrm{kg/m^3} \quad (18)$$

The confidence bounds (95%) of the density random error are equal to ±0.08%. In this temperature range, the sample represents an intermixture of β' and Mg_2Pb phases. As the thermal expansion coefficient calculated from Eq. (18) is less than that calculated from Eq. (17) on 15%, it is possible to conclude that the CTE of the β'-phase is a little less than that of the Mg_2Pb phase.

Data fitting for the alloy with 52.46 at.% Pb content has given the following equation:

$$\rho_{FD}(T) = 7252 - 0.50501\,(T - 20\ ^{\circ}\mathrm{C})\ \text{in}\ \mathrm{kg/m^3} \quad (19)$$

The confidence bounds (95%) of the density random error are equal to ±0.05%. As well as for 33.45 at.% Pb composition the total error of the density is much higher because of the liquation. The mean values of the volume changes on phase transitions are equal to:

$$\delta\rho_{CL} = (3.85 \pm 0.15)\%,\ \delta\rho_{EC} = -(4.15 \pm 0.30)\%,\ \delta\rho_{DE} = (1.25 \pm 0.15)\% \quad (20)$$

These data show that the density of the β′-phase is at least 4% more than Mg_2Pb density.

A comparison of the density of the alloys obtained in the solid state with their additive values ρ_{AD} represents a practical interest. The calculated values of ρ_{AD} for the samples with 33.45 and 52.46 at.% Pb composition are 2.8 and 2.2% more than the experimental values, respectively, if pure magnesium and lead (density from [5] and [8]) are considered the components. If the sample with 52.46 at.% Pb composition is considered as a mixture of pure lead and Mg_2Pb (density from Eq. (17)), the additive value is only 0.36% less than the measured density. Thus, it is possible to expect that the additive approach will give reliable and precise results for other compositions if the Mg_2Pb phase is considered as one of the components.

4. Conclusion

The present investigation has shown that the gamma method of phase analysis allows to obtain reliable data on the temperatures of the phase equilibriums of multicomponent systems in both the solid and liquid states. In comparison with a thermal analysis, this method has some advantages, which include the possibility of carrying out measurements at small heating/cooling rates (including zero), controlling the homogeneity of the sample, and obtaining data on the density and thermal expansion coefficients. The measurements of the temperatures of the phase equilibria in the magnesium–lead system have shown that the standard phase diagram of this system contains inaccuracy in the region of the Mg_2Pb intermetallic compound. The possible reason is the poor homogenization of the samples, which does not allow the division of the heat effects because of a small difference between the peritectic reaction temperature and the liquidus temperature.

Acknowledgement

We gratefully thank the Russian Foundation for Basic Research (Grant No. 06-08-00040) for providing the financial support for this research.

References

[1] A.A. Nayeb-Hashemi, J.B. Clark, Bull. Alloy Phase Diagrams 6 (1985) 56–66.
[2] N.P. Lyakishev, Phase Diagrams of Binary Metallic Systems, Mashinistroenie, Moscow, 2001 (in Russian).
[3] J.M. Eldridge, E. Miller, K.L. Komarek, Trans. AIME 233 (1965) 1304–1308.
[4] N.G. Siviour, K. Ng, Metall. Mater. Trans. 25B (1994) 265–275.
[5] S.V. Stankus, R.A. Khairulin, Tsvetnye Metally No. 9 (1990) 65–67.
[6] S.V. Stankus, P.V. Tyagel'sky, J. Cryst. Growth 167 (1996) 165–170.
[7] R.A. Khairulin, S.V. Stankus, High Temp. High Press. 32 (2000) 193–198.
[8] S.V. Stankus, R.A. Khairulin, High Temp. 44 (2006) 393–400.
[9] D.J. Hudson, Statistics, CERN, Geneva, 1964.
[10] S.V. Stankus, R.A. Khairulin, P.V. Tyagel'sky, Thermophys. Aeromech. 11 (2004) 153–159.
[11] G. Brauer, J. Tiesler, Z. Anorg. Chem. 262 (1950) 319–327.
[12] J.M. Eldridge, E. Miller, K.L. Komarek, Trans. AIME 239 (1967) 775–781.
[13] R.A. Khairulin, A.S. Kosheleva, S.V. Stankus, Thermophys. Aeromech. 14 (2007) 75–80.